Using High Rydberg States as Electric Field Sensors

A. Osterwalder and F. Merkt
Laboratorium für Physikalische Chemie, ETH-Zürich, CH-8092 Zürich, Switzerland
(Received 30 October 1998)

High Rydberg states of the krypton atom have been investigated at high resolution by vacuum ultraviolet–millimeter wave double-resonance spectroscopy. The measurement of Stark shifts in the spectra of these high Rydberg states is used to determine electric fields with a ± 20 μV/cm accuracy. The analysis of spectral line shapes provides information on inhomogeneous electric field distributions in the experimental volume. [S0031-9007(99)08605-6]

PACS numbers: 32.60.+i, 32.30.Bv, 32.70.Jz, 32.80.Wr

High Rydberg states display an unusual sensitivity to electric fields: The polarizability of an atom in a Rydberg state of principal quantum number n is proportional to n^7, and the threshold field for field ionization is proportional to n^{-4} [1]. Spectroscopic measurements on high Rydberg states can only be performed at very low electric fields. For example, Neukammer *et al.* [2] had to reduce their electric fields to less than 45 μV/cm to obtain spectra of barium Rydberg states at $n = 520$. The very rapid variation of their properties with n renders high Rydberg states attractive as electric field sensors: Even a small electric field leads to a substantial change in the properties of sufficiently high Rydberg states. Recent studies have demonstrated that a quantification of this change enables accurate measurements of electric fields [3–5].

Hotop and co-workers [4,5] diagnosed and reduced electric fields to levels around 100 μV/cm by monitoring SF_6^- formation around the onset of field ionization of high n Rydberg states of the argon atom. Their diagnostic method relies on the observation of a discontinuity in the SF_6^- yield at the field ionization onset [5]. Its sensitivity results from the very rapid decrease (with n^{-4}) of the threshold fields for ionization at increasing n values.

Frey and co-workers [3] measured and subsequently minimized electric fields to less than 50 μV/cm by exploiting the Stark effect. To measure the fields, a high resolution laser was detuned a few MHz to the red of a particular $4s \rightarrow np$ transition in alkali atoms. The magnitude of a bias voltage applied between a pair of opposing electrodes was varied until the transition frequency was brought into resonance with the laser frequency, at which point efficient absorption led to the observation of a large field ionization signal. Because the energy shift of a Rydberg state undergoing a quadratic Stark effect is proportional to the polarizability, which itself grows as n^7, the sensitivity of this electric field measurement improves rapidly with n.

Both methods described above are ideally suited to precisely determine and compensate *homogeneous* electric fields but do not provide information on *inhomogeneous* electric fields, such as those caused by charged particles, or dipolar molecules that may be present in the experimental volume. These procedures are therefore not suited to gain a complete picture of the stray fields in situations where ion concentrations are not negligible, as is typically the case in pulsed field ionization zero kinetic energy spectroscopy [6–8] or in spectroscopic measurements in ultracold samples [9,10]. Controlling homogeneous and inhomogeneous stray electric fields may also be important for coherent quantum-state manipulation of trapped ions [11].

The method reported here to determine stray electric fields relies on the same principle as the second field measurement method described above. However, instead of measuring the resonant electric field by sweeping the bias voltage at a fixed excitation frequency, spectra are recorded by scanning the excitation frequency at fixed electric field values. This procedure has the advantage that additional information on the *inhomogeneous* electric field distribution in the experimental volume can be extracted from the shape of the spectral lines. In experimental situations like the present one, where the photoexcitation volume is small compared to the dimensions of the apparatus and well removed from any surface material, the stray electric fields that originate from rest or patch surface potentials are, to a good approximation, homogeneous. Stray field inhomogeneities are caused almost entirely by charged or dipolar particles located within the probe volume and can be analyzed in terms of the Holtsmark distribution functions [12,13].

Experiment.—High-resolution spectra of high Rydberg states are measured by the vacuum ultraviolet (vuv)–millimeter wave double-resonance method described in Ref. [14]. A broadly tunable (65–130 nm), narrow bandwidth (0.1 cm^{-1}) pulsed vuv laser [15] is used to induce a transition from the ground neutral state of an atom or a molecule in a skimmed supersonic beam to a selected Rydberg state in the range $n = 50$–150. Transitions from this Rydberg state to higher lying Rydberg states are induced by a tunable (120–180 GHz) source of millimeter waves and detected by selective delayed pulsed field ionization of the upper Rydberg states. Photoexcitation is carried out in a 5.7 cm long, magnetically shielded (shielding coefficient of 5000) region surrounded by cylindrical electrodes across which dc bias voltages can be applied. For the experiments described in this Letter

the vuv laser was held fixed at the frequency of the $(4p)^6\,{}^1S_0 \rightarrow (4p)^5 77d[3/2](J = 1)$ transition in krypton and the millimeter waves were used to record spectra of the region around the $n = 91$ Rydberg states. Spectral resolution improves with increasing delay time between laser and electric field pulse (i.e., at increasing interaction time of the millimeter waves with the atoms). This is illustrated in Fig. 1 which shows millimeter wave spectra of the $77d[3/2](J = 1) \rightarrow 93p[3/2](J = 1)$ transition recorded using delay times in the range between 1 and 18 μs. The ultimate resolution of 60 kHz achieved in our apparatus is limited by the transit time of 12–18 μs of the excited molecules through the region of interaction with the millimeter waves.

Results.—The high sensitivity of high Rydberg states to electric fields is illustrated in Fig. 2, which shows the onset of the Stark effect at $n = 91$. The spectra have been recorded by applying dc bias voltages on the extraction plates so as to generate electric fields in the range 0–44 mV/cm. At zero field [trace (a)] only three lines are observed corresponding to the three fine structure components of the $91f$ state that are optically accessible from the selected intermediate $77d[3/2](J = 1)$ state [in order of increasing frequency $91f[3/2](J = 1)$, $91f[3/2](J = 2)$, and $91f[5/2](J = 2)$]. These states undergo a quadratic Stark effect at low fields [traces (a)–(d)]. As the field increases, the spectra first reveal the appearance of the g Rydberg states [trace (b)] that become observable as a consequence of Stark mixing with the f states. At fields above $\approx$10 mV/cm, the high l states which undergo a linear Stark effect progressively gain in importance until the f states are completely absorbed by the linearly expanding high l manifold of Stark states [trace (g)]. Important observations, discussed below, are that transitions to states located at the center of the linear Stark manifold are very sharp and that a gradual broadening becomes noticeable as one moves toward either edge of the Stark manifold [traces (e)–(g)].

Figure 3 illustrates how the homogeneous components of the stray electric fields are measured and compensated using the $77d[3/2](J = 1) \rightarrow 91f[5/2](J = 2)$ transition as an example. The transition is recorded at several positive and negative bias voltages on the extraction plates. For the graphical representation, the spectra have been shifted along the vertical axis by an offset corresponding to the value of the applied electric field $F_{z,\mathrm{applied}}$. Because the Stark shift is proportional to the square of the magnitude of the electric field but does not depend on its sign, the line centers of the different measurements lie on a parabolic curve of the form

$$\nu = \nu_0 + c(F_{z,\mathrm{applied}} + F_{z,\mathrm{stray}})^2 + c(F_{y,\mathrm{stray}}^2 + F_{x,\mathrm{stray}}^2), \quad (1)$$

where ν_0 corresponds to the zero field transition frequency and c is a constant. The apex of the parabola, which corresponds to the point $[\nu_{0,z} = \nu_0 + c(F_{y,\mathrm{stray}}^2 + F_{x,\mathrm{stray}}^2), F_{z,\mathrm{applied}} = -F_{z,\mathrm{stray}}]$, can be determined accurately from a fit of the line centers to Eq. (1). For the measurement displayed in Fig. 3, the fit yields $F_{z,\mathrm{stray}} = -646 \pm 20\ \mu\mathrm{V/cm}$ and $\nu_{0,z} = 174\,779.016 \pm 0.015$ MHz. The stray field component along the z axis can subsequently be reduced to less than 20 μV/cm by applying a dc bias field of $+646\ \mu$V/cm. The procedure can be repeated for the x and y directions.

A gradual broadening of the transitions is noticeable at increasing field strength in Fig. 3. This broadening has the same origin as that observed in traces (e)–(g) of Fig. 2: It results from the inhomogeneous electric field distribution in the sample volume, as is illustrated

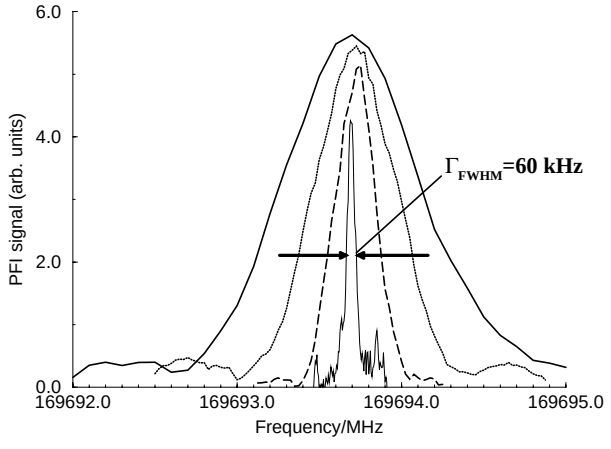

FIG. 1. Millimeter wave spectra of the $77d[3/2](J = 1) \rightarrow 93p[3/2](J = 1)$ transition recorded using delay times of 1 (full bold line), 1.5 (dotted line), 3 (dashed line), and 18 μs (thin full line) between laser pulse and PFI.

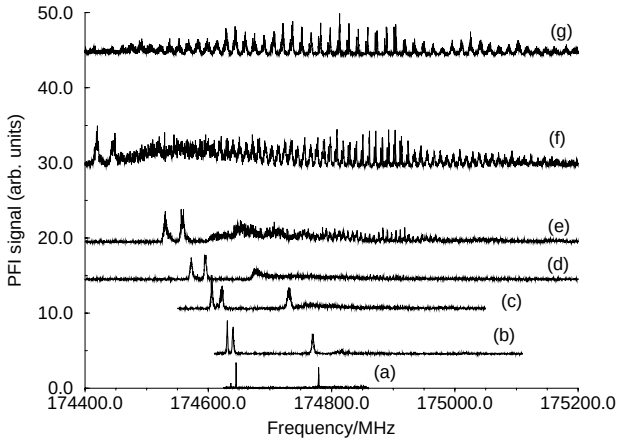

FIG. 2. Stark spectra of krypton at $n = 91$ recorded following vuv–millimeter wave double-resonance excitation via the $77d[3/2](J = 1)$ intermediate state. The spectra have been shifted along the vertical axis by an offset corresponding to the value of the applied electric field: (a) 0 mV/cm; (b) 4.56 mV/cm; (c) 10.57 mV/cm; (d) 14.53 mV/cm; (e) 19.43 mV/cm; (f) 29.45 mV/cm; and (g) 44.43 mV/cm.

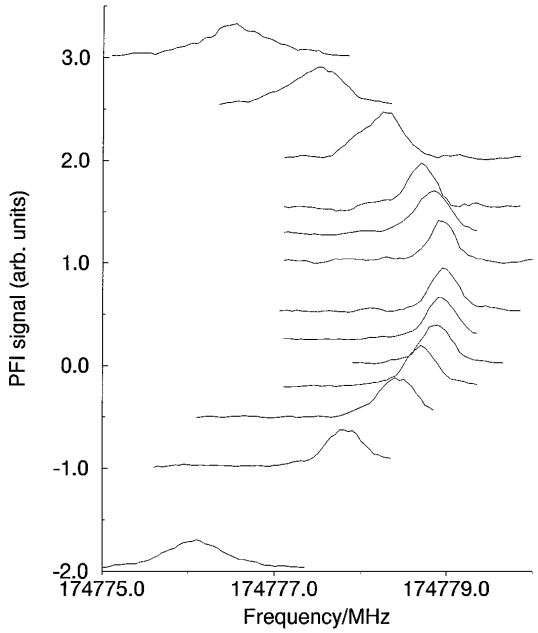

FIG. 3. Stark spectra of the $77d[3/2](J = 1) \rightarrow 91f[5/2](J = 2)$ transition. The spectra have been shifted along the vertical axis by an offset corresponding to the value of the applied electric field (from top to bottom: 2.99, 2.51, 1.98, 1.52, 1.26, 0.99, 0.50, 0.23, 0, −0.23, −0.52, −0.99, and −1.98 mV/cm).

schematically in Fig. 4. The figure represents the field dependence of the energetic levels of Rydberg states undergoing a quadratic [Fig. 4(a)] and a linear [Fig. 4(b)] Stark effect. Because of inhomogeneities in the electric field distribution, the actual value of the electric field varies across the sample volume in a range represented schematically by two vertical dashed lines on both sides of the central field value (F_1 or F_2 in Fig. 4). Consequently, the Rydberg states probed experimentally are all subject to slightly different electric fields and display different Stark shifts. For Rydberg states subject to a quadratic Stark effect, the broadening that results from the same inhomogeneous electric field distribution is more pronounced at larger electric fields [see Fig. 4(a)]. In addition, the lines can be predicted to be asymmetrically broadened and degraded to the low (high) frequency side for a red (blue) shifted Stark state (see also Fig. 5). In contrast, the slope of Rydberg states undergoing a linear Stark effect is independent of the electric field strength and so are the inhomogeneous broadenings. However, the broadenings are expected to be large for Stark states located at the edge of the Stark manifold (these states display a strong field dependence) but negligible for Stark states located at the center of the manifold [Fig. 4(b)], as is observed experimentally (see Fig. 2).

Figure 5 demonstrates that the broadening that results from the electric field inhomogeneities strongly depends on the laser power. The upper panel shows three spectra of the $77d[3/2](J = 1) \rightarrow 91f[5/2](J = 2)$ transition recorded at laser powers of $\leq 10^6$, $\approx 5 \times 10^6$, and $\approx 2.5 \times 10^7$ photons/pulse, respectively. At increasing laser power, the line shape undergoes a marked asymmetric broadening towards lower frequencies. Because the vuv laser pulse duration of 5 ns is negligible compared to the delay time of several microseconds used to drive the millimeter wave transitions, one can safely rule out that the broadening originates from the oscillating laser field. The change of line shape can be attributed only to ions or Rydberg states initially excited by the laser. At the end of the laser pulse the majority of excited species are $77d[3/2](J = 1)$ Rydberg states, although ions are also produced by direct ionization of krypton clusters in the beam and of water molecules in the background and by collisional and associative ionization, as well as millimeter wave ionization, of the initially prepared $77d[3/2](J = 1)$ Rydberg states. Preliminary estimates suggest that, despite their smaller concentration, the role of ions in the line broadening is more important than that of the initially prepared $n = 77$ Rydberg states. Figure 5(b) shows line shapes calculated on the basis of Holtsmark's field distributions [12] for different concentrations of ions in the sample volume. The full, dotted, dash-dotted, and dashed lines in Fig. 5(b) were obtained

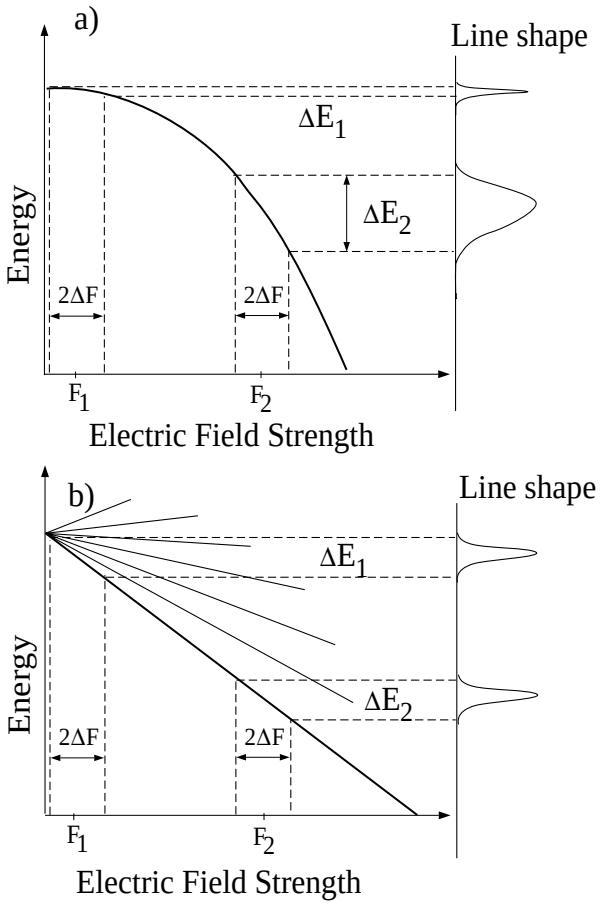

FIG. 4. Inhomogeheous broadening in Rydberg states undergoing a quadratic (a) and a linear (b) Stark effect.

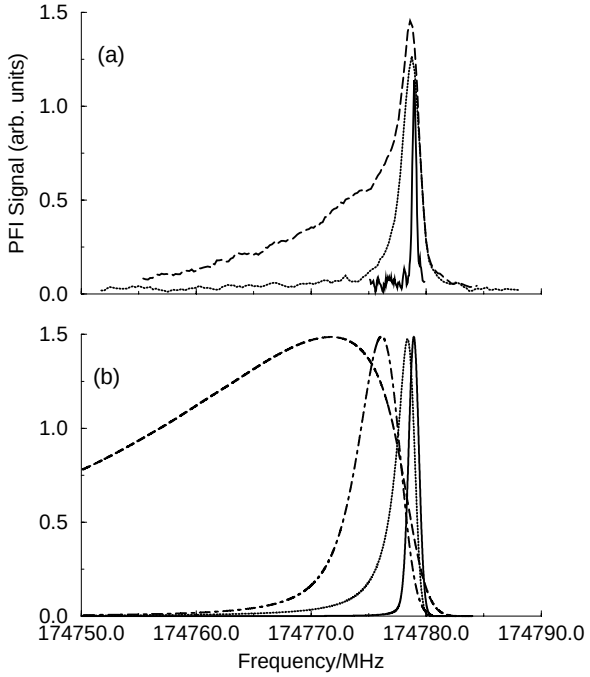

FIG. 5. (a) Line shape of the $77d[3/2](J = 1) \rightarrow 91f[5/2](J = 2)$ transition recorded at different laser intensities. The full, dotted, and dashed lines were recorded using laser power of $\leq 10^6$, $\approx 5 \times 10^6$, and $\approx 2.5 \times 10^7$ photons/pulse, respectively. (b) Line shapes predicted using Holtsmark's field distribution for ion concentration of 10^4 (full line), 10^5 (dotted line), 3×10^5 (dash-dotted line), and 10^6 ions/cm^3 (dashed line), respectively.

by assuming concentrations of 10^4, 10^5, 3×10^5, and 10^6 ions/cm^3, respectively. Although the calculated line shapes qualitatively reproduce the observed line shapes, some marked differences (particularly at the highest laser power) necessitate further investigations. A more elaborate modeling of the line shapes would have to take into account the fact that the ion concentration increases during the experimental observation time and include the effect of other Rydberg states.

In conclusion, high Rydberg states can be used as sensors for very small electric fields. By measuring line shifts in the spectra of high Rydberg states, it is possible to measure homogeneous electric fields very accurately and to subsequently reduce them to less than 20 μV/cm. By analyzing the inhomogeneous broadening observed in the spectra of high Rydberg states, important information can be gained on inhomogeneous electric field distributions in the sample volume. In favorable cases, these field distributions can be related to the concentration of charged particles in the experimental volume.

This work was supported by the ETH-Zürich.

[1] T. F. Gallagher, *Rydberg Atoms* (Cambridge University Press, Cambridge, 1994).
[2] J. Neukammer, H. Rinneberg, K. Vietzke, A. König, H. Hieronymus, M. Kohl, H.-J. Grabka, and G. Wunner, Phys. Rev. Lett. **59**, 2947 (1987).
[3] M. T. Frey, X. Ling, B. G. Lindsay, K. A. Smith, and F. B. Dunning, Rev. Sci. Instrum. **64**, 3649 (1993).
[4] H. Hotop, D. Klar, M.-W. Ruf, A. Schramm, and J. M. Weber, in *The Physics of Electronic and Atomic Collisions*, AIP Conf. Proc. No. 360 (AIP, New York, 1995), p. 267.
[5] A. Schramm, J. M. Weber, J. Kreil, D. Klar, M.-W. Ruf, and H. Hotop, Phys. Rev. Lett. **81**, 778 (1998).
[6] K. Müller-Dethlefs and E. W. Schlag, Annu. Rev. Phys. Chem. **42**, 109 (1991).
[7] W. A.Chupka, J. Chem. Phys. **98**, 4520 (1993).
[8] F. Merkt and R. N. Zare, J. Chem. Phys. **101**, 3495 (1994).
[9] I. Mourachko, D. Comparat, F. de Tomasi, A. Fioretti, P. Nosbaum, V. M. Akulin, and P. Pillet, Phys. Rev. Lett. **80**, 253 (1998).
[10] W. R. Anderson, J. R. Veale, and T. F. Gallagher, Phys. Rev. Lett. **80**, 249 (1998).
[11] D. J. Wineland, C. Monroe, W. M. Itano, D. Leibfried, B. E. King, and D. M. Meekhof, J. Res. Natl. Inst. Stand. Technol. **103**, 259 (1998).
[12] J. Holtsmark, Ann. Phys. (Leipzig) **58**, 577 (1919).
[13] J. Holtsmark, Phys. Z. **25**, 73 (1924).
[14] F. Merkt and H. Schmutz, J. Chem. Phys. **108**, 10 033 (1998).
[15] F. Merkt, A. Osterwalder, R. Seiler, R. Signorell, H. Palm, H. Schmutz, and R. Gunzinger, J. Phys. B **31**, 1705 (1998).